

PLASMA ANODIZATION OF EVAPORATED Al-InP SYSTEMS

Y. Hirayama, H. M. Park, F. Koshiga and T. Sugano

Department of Electronic Engineering,
The University of Tokyo,
3-1, Hongo 7 chome, Bunkyo-ku, Tokyo, 113 Japan

(Received May 5, 1982)

Aluminium oxide-InP structures were fabricated by plasma anodization of evaporated Al-InP systems with intention of fabricating InP MISFETS. It was found that the resistivity and break-down strength of the Al_2O_3 film were influenced by the selection of the end point of the anodization. At appropriate conditions the resistivity of $5 \times 10^{10} - 10^{12} \Omega \text{ cm}$ for the anodic Al_2O_3 and the minimum density of the interface trap states of $4 \times 10^{11} \text{ cm}^{-2} \text{ ev}^{-1}$ for Al_2O_3 -InP systems were obtained.

Key words: plasma anodization, InP, MIS diode, Al_2O_3 .

Introduction

Anodization of a deposited metal film is one of the useful technologies to form an insulating layer on the surface of a semiconductor substrate, whose temperature must be maintained at low temperature during processing in order to avoid deterioration of the surface. Some results have been reported about the properties of anodic Al_2O_3 -GaAs structure (1-3). However, neither surface accumulation nor inversion can be attained in anodic Al_2O_3 -GaAs systems. In contrast with GaAs, it is possible

to induce both a strong inversion layer on the surface of p type InP substrate as well as a strong accumulation layer on the surface of n type and semi-insulating InP substrate. Enhancement-mode field effect transistors on both p type and semi-insulating substrates have already been fabricated using pyrolytic SiO_2 (4-6), Al_2O_3 (7,8), plasma assisted chemical vapor deposited SiO_2 (9), Si_3N_4 (9), anodic Al_2O_3 (10), and other films (11, 12) as the gate insulators.

Anodization in an oxygen plasma is a promising low temperature dry process technology because of its good controllability and no contamination of the grown oxide film. The good controllability of plasma anodization process is due to no back dissolution of the anodized film which happens in electrochemical anodization. The SiO_2 (13) and GaAs (14) native oxide with good quality have been grown by plasma anodization at low temperature.

In this work Al_2O_3 -InP structures were fabricated by plasma anodization of evaporated Al-InP systems with the intention of fabricating InP MISFETs(15, 16). Electrical properties of plasma anodic Al_2O_3 film on InP substrate were investigated in relation to the end point of anodization. The capacitance-voltage (C-V) characteristics of Al-plasma anodic Al_2O_3 -InP metal-insulator-semiconductor (MIS) diode were also investigated.

Experimental results and discussions

Plasma anodization of evaporated Al-InP structure

An aluminium film with a thickness of 250 Å deposited on the surface of an InP substrate at the deposition rate of 5 Å/sec. Before deposition of Al the InP surface was chemically etched in Br (2%)-methanol, then dipped into 7 % HCl and deionized water, successively.

Plasma anodic oxidation of evaporated Al films on InP substrates was performed at an anodization current density of 6 mA/cm², in an oxygen atmosphere of 0.1 Torr, and the substrate temperature during anodization was between 150°C and 180°C. The substrate temperature was controlled by either changing the position of the substrate in the oxy-

gen plasma and the rf power to generate the plasma. The oxygen gas was moistened by passing it through a deionized water bubbler, in order to improve the uniformity of the Al_2O_3 film in breakdown voltage. The change of the terminal voltage during plasma anodic oxidation is shown in Fig.1. The curve shows that the terminal voltage saturates after anodization of Al on the surface of InP, because the anodization rate of the InP substrate was very small under these anodization conditions. **

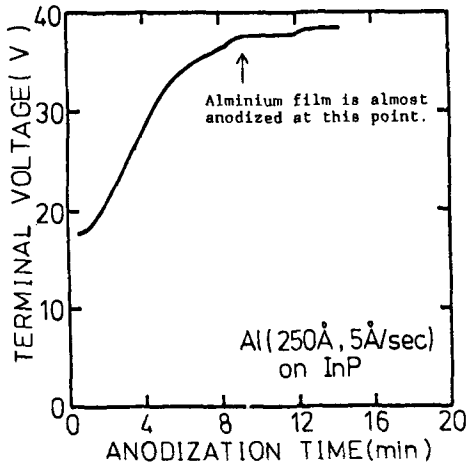


Fig. 1. The change of the terminal voltage during plasma anodic oxidation. The terminal voltage is the dc voltage between the anode and the cathode when constant anodization current is flowing. The increase of the terminal voltage saturates after finishing anodization of Al on the surface of InP.

After plasma anodization, annealing was carried out in argon for one hour at 250°C . Figure 2 indicates that the annealing is a useful procedure for reducing the anomalous characteristics and hysteresis of C-V curve. Annealing in an atmosphere containing hydrogen or at temperature above 300°C results in a higher density of interface trap states in comparison with annealing in argon at 250°C .

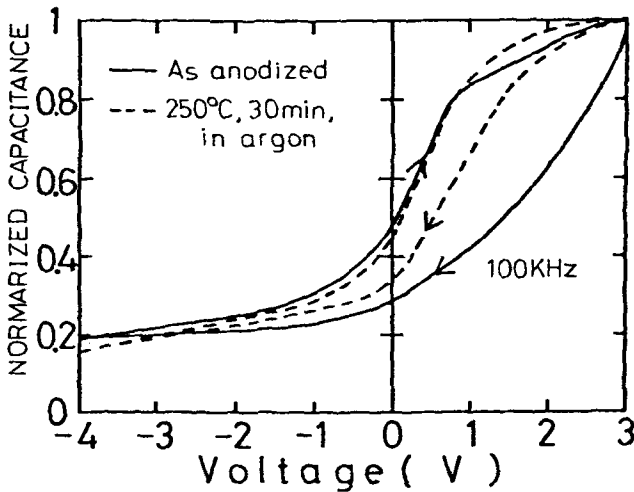


Fig. 2. The change of C-V characteristics of Al-plasma anodic Al_2O_3 -InP MIS diode by annealing. The annealing in argon ambient for one hour at 250°C reduces the anomalous characteristics of C-V curves.

Table 1 Typical properties of plasma anodic Al_2O_3 on InP substrate.

	Time of anodization after saturation	
	2-3 min	12-15 min
thickness	630Å	860Å
refractive index (6328 Å)	1.72	1.68
resistivity ($2 \times 10^{-6} \text{A/cm}^2$)	$5 \times 10^{10} \sim 10^{12} \Omega \cdot \text{cm}$	$3 \times 10^9 \sim 2 \times 10^{10} \Omega \cdot \text{cm}$
dielectric constant	~ 7	~ 6
breakdown strength	$1.2 \sim 1.6 \times 10^6 \text{V/cm}$	$0.8 \sim 1 \times 10^6 \text{V/cm}$

The thickness of the aluminium film was about 250Å and deposition rate of aluminium was 5Å/sec .

Properties of Al₂O₃ film on InP substrates

Typical properties of the Al₂O₃ films are summarized in Table.1. These properties were measured for an Al₂O₃ film formed on an n-type InP substrate whose carrier concentration was about 10¹⁸cm⁻³. The thickness and refractive index of the Al₂O₃ films were measured by means of ellipsometry assuming the formation of a transparent homogeneous oxide film on the InP substrates. The refractive index 3.43 - 0.3 j was assumed (17,18). The dielectric constant was estimated from the capacitance of MIS structures. The resistivity of 10¹¹ - 10¹²Ωcm is small compared with CVD films (6, 7, 19) but two order of the magnitude larger than plasma anodized native oxide film on InP (20). The dielectric constant is slightly small compared with CVD Al₂O₃ film (7).

In spite of the saturation of the terminal voltage, the characteristics of the Al₂O₃ film change with the end point of anodization. When anodization was continued for a long time after saturation, the resistivity and breakdown strength of the Al₂O₃ film became small.

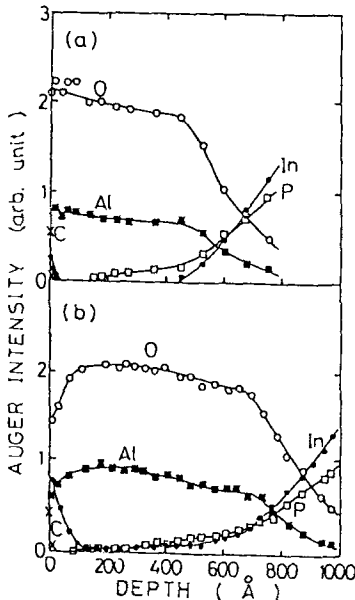


Fig. 3. The Auger in-depth profiles of plasma anodic Al₂O₃ on InP substrate. The anodization was finished 2-3 minutes(a) and 12-13 minutes(b) after saturation of the terminal voltage. The large amount of In incorporation into the Al₂O₃ film is observed in Fig.3(b).

The Auger depth profiles of plasma anodic Al_2O_3 film are shown in Fig.3. Figure 3(a) shows the profile of the Al_2O_3 film whose anodization was finished 2-3 minutes after saturation of terminal voltage. The In incorporation into the Al_2O_3 film is small. Figure 3(b) shows the profiles of the Al_2O_3 film whose anodization was finished 12-13 minutes after saturation. The peak to peak height of the Auger signal of each species is plotted. The In, P, Al, and O Auger lines originate from MNN, LMM, LMM, and KLL transitions, respectively. The primary electron beam energy is 10 KeV and the beam current is $2\mu\text{A}$. The energy resolution ($\Delta E/E$) is 0.5%. The sputter-etching was carried out using 5 keV Ar ion beam and the uniform sputter-etching rate was assumed upto the interface between the Al_2O_3 film and the InP substrate for each sample. The sputter-etching rates were about 14 A/min for Fig. 3(a) and about 8 A/min for Fig.3 (b). Carbon which was detected for the first few seconds of sputter-etching was due to contamination of the surface. In the anodization continued for a long time after saturation of the terminal voltage, then it appears that larger amount In and P atoms migrated into Al_2O_3 film and the sputter-etching rate of the Al_2O_3 decreased. In both figures a pile up of In atoms at the surface region of the Al_2O_3 film is found, but excess P atoms at the surface region is not detected. This suggests that P atoms have been dissociated from the surface during the plasma anodization.

Figure 4 shows the change of the Auger lines of In and P through the sputtering time of the Al_2O_3 film whose profiles are shown in Fig.3(b). The parameter is the depth from the surface. The depths of 300 Å and 530 Å correspond to the bulk Al_2O_3 region. The Auger lines of the InP substrate are also shown in Fig.4. At the surface of the Al_2O_3 film ($d=0$ Å) P was not detected. Since the chemical bonding between In and P is relatively weak, the chemical shift of the In and P lines in InP is small. On the other hand, when In and P bond to O the Auger line shifts to a lower energy substantially(21-23). Figure 4 shows that this shift is observed in the bulk Al_2O_3 region for P but is observed only at the surface region for In. This means that P atoms in the Al_2O_3 film bond to O but most of In atom in the bulk Al_2O_3 film are not bond to O. Incorporation of unoxidized In atoms into the Al_2O_3 film is thought to be the cause of the electrically leaky property of the

Al_2O_3 film whose anodization was continued for a long time after saturation of the terminal voltage. In consequence, it is necessary to finish the anodization only a few minutes after the saturation of terminal voltage to obtain an Al_2O_3 film with high resistivity.

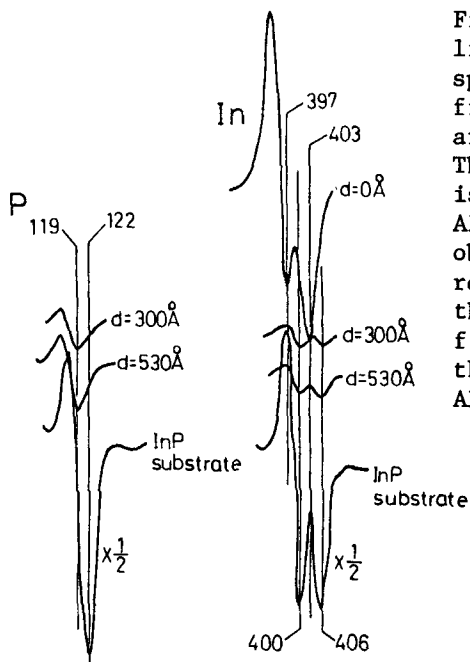


Fig. 4 The change of Auger lines of In and P with the sputtering time. The profiles of this Al_2O_3 film are shown in Fig.3(b). The Auger chemical shift is observed in the bulk Al_2O_3 region for P but observed only at the surface region for In. This means that P atoms in the Al_2O_3 film bond to O but most of the In atoms in the bulk Al_2O_3 film do not bond to O.

The room temperature current-voltage characteristics of Al- Al_2O_3 -InP MIS diode whose anodization was finished at the appropriate point is shown in Fig.5. The current flow mechanism through the Al_2O_3 film can be understood in terms of a Poole-Frenkel mechanism. From the slope of the straight line the dynamic dielectric constant is estimated to be 4.8.

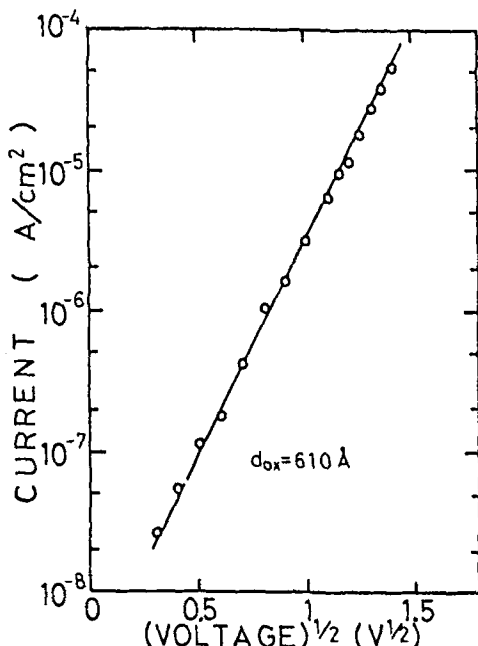


Fig. 5. Current vs bias characteristics of Al-plasma anodic Al_2O_3 -InP MIS diode. The current flow mechanism through Al_2O_3 film can be understood by the Poole-Frenkel mechanism.

The capacitance-voltage (C-V) characteristics

The C-V characteristics of an MIS diode are shown in Fig.6. The thick Al film with area about $1 \times 10^3 \text{ cm}^2$ was deposited as the field electrode. The C-V characteristics have hysteresis as shown in Fig.2, but the curves in Fig.6 were measured by scanning the bias voltage from positive to negative. The C-V curves show slightly larger hysteresis at 77K than at room temperature. In the dark condition, the low temperature precludes the generation of minority carriers so that a deep depletion curve is observed. Under illumination, minority carriers which are optically generated at the region surrounding the field electrode flow into the depleted region below the field electrode and the capacitance in the negative bias region is pinned at the onset of inversion. This value is in good agreement with the calculated value from the doping density for this substrate. Figure 6 shows that the interface potential can be swept over the entire range of the band gap of InP at room temperature and 77K.

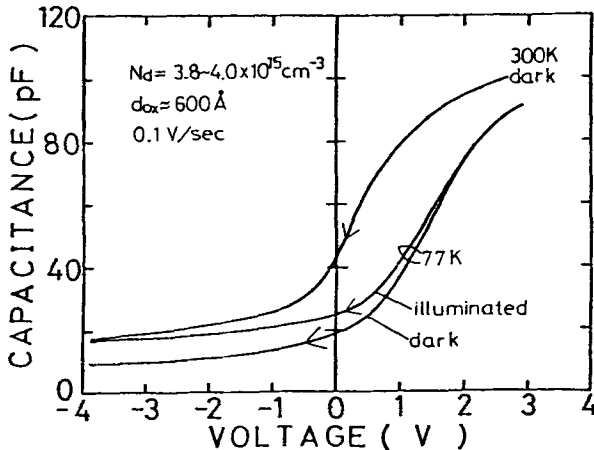


Fig. 6. C-V characteristics of Al-plasma anodic Al_2O_3 -InP MIS diode. This figure shows that the interface potential can be swept for the entire range of the band gap of InP at both room temperature and 77K. Only the result of a unidirectional scan is shown in this figure.

The minimum densities of the interface trap states calculated by Terman method (24) are $4 \times 10^{11} \text{ cm}^{-2} \text{ eV}^{-1}$ at room temperature and $9 \times 10^{10} \text{ cm}^{-2} \text{ eV}^{-1}$ at 77K (14). The decrease of the density of the interface trap states is thought to be due to slow response of interface trap states at low temperature. The density of interface trap states is almost of the same order of the magnitude as that of dielectric-InP systems prepared by the other method, such as CVD SiO_2 (19).

Conclusions

Al_2O_3 -InP structures have been fabricated by the anodization of deposited Al-InP structure in an oxygen plasma. The characteristics of Al_2O_3 on InP substrate were found to be influenced by the selection of the end point of anodization. When anodization was continued for a long time after the saturation of the terminal voltage, In atoms which were not oxidized incorporated into the Al_2O_3 film and the Al_2O_3 film becomes electrically leaky. When the anodization was

finished a few minutes after saturation, an Al_2O_3 film with high resistivity was obtained.

The C-V characteristics of Al-plasma anodic Al_2O_3 -InP MIS diode show that the interface potential can be swept over the entire range of the band gap of InP. The density of the interface trap states are about $10^{12}\text{cm}^{-2}\text{eV}^{-1}$ for the almost entire band gap and the minimum density of the interface trap states is $4 \times 10^{11}\text{cm}^{-2}\text{eV}^{-1}$ at room temperature.

Acknowledgements

We would like to thank Sumitomo Electric Co. Ltd. for supplying InP wafers to us.

*Aluminium oxide will be described as Al_2O_3 in this paper.
**The anodization rate of InP was very small in this work, but the direct plasma anodization of InP was reported by K.Kanazawa and H. Matsunami (20) using oxygen plasma with magnetic confinement.

References

1. D.W. Langer, F.L. Schuermeyer, R.L. Johnson, H.P. Singh, C.W. Litton and H.L. Hartnagel, J. Vac. Sci. Technol. 17, 964 (1980).
2. H. Hayashi, K. Kikuchi, and T. Yamaguchi, Appl. Phys. Lett. 37, 404 (1980).
3. Y. Hirayama, F. Koshiga, and T. Sugano, J. Appl. Phys. 52, 4697 (1981).
4. D.L. Lile, D.A. Collins, L.G. Meiners, and L. Messick, Electron. Lett. 14, 657 (1978).
5. L.G. Meiners, D.L. Lile, and D.A. Collins, Elelectron. Lett. 15, 578 (1979).
6. D. Fritzsche, Inst. Phys. Conf. Ser. 50, 258 (1979).

7. T. Kawakami and M. Okamura, *Electron. Lett.* 15, 502 (1979).
8. T. Kawakami and M. Okamura, *Electron. Lett.* 15, 743 (1979).
9. J. Woodward, D.C. Cameron, L.D. Irving, and G.R. Jones, *Thin Solid Films* 85, 61 (1981).
10. T. Sawada, K. Ishii, and H. Hasegawa, *Japan. J. Appl. Phys. Suppl.* 21-1, 397 (1982).
11. L. Henry, D. Lecrosnier, H. L'Haridon, J. Paugam, G. Pelous, F. Richou and M. Salvi, *Electron. Lett.* 18, 102 (1982).
12. A. Yamamoto and C. Uemura, *Electron. Lett.* 18, 63 (1982).
13. V.Q. Ho and T. Sugano, *IEEE Trans. Electron Dev.* ED-28, 1060 (1981).
14. K. Yamasaki and T. Sugano, *Japan. J. Appl. Phys. Suppl.* 17-1, 321 (1981).
15. Y. Hirayama, H.M. Park, F. Koshiga and T. Sugano, *Inst. Phys. Conf. Ser.* 63, 431(1982).
16. Y. Hirayama, H.M. Park, F. Koshiga and T. Sugano, *Appl. Phys. Lett.* 40, 712 (1982).
17. R.K. Willardson and A.C. Beer (Eds.), "Semiconductors and Semimetals", 3, Academic, New York, 1967.
18. H. Burkhard et al., *J. Appl. Phys.* 53, 655 (1982).
19. L. Messick, *J. Appl. Phys.* 47, 4949 (1976).
20. K. Kanazawa and H. Matsunami, *Japan. J. Appl. Phys.* 20, L211 (1981).
21. C.W. Wilmsen and R.W. Kee, *J. Vac. Sci. Technol.* 14, 953(1977).
22. C.W. Wilmsen and R.W. Kee, *J. Vac. Sci. Technol.* 15, 1513 (1978).

23. J.F. Wager and C.W. Wilmsen, submitted to J. Appl. Phys.

24. L.M. Terman, Solid State Electronics 5, 285 (1962).